

## Electrodeposition of cerium conversion coatings for corrosion protection of D16 AM clad alloy

J. A. P. Ayuso<sup>1</sup>, S. Kozhukharov<sup>2\*</sup>, M. Machkova<sup>2</sup>, V. Kozhukharov<sup>2</sup>

<sup>1</sup>University of Vigo, Lagoas, Marcosende 36310 (Spain)

<sup>2</sup>University of Chemical Technology and Metallurgy, 8 “Kl. Okhridsky” Blvd., Sofia 1756 (Bulgaria)

Received January 31, 2013; Revised May 21, 2013

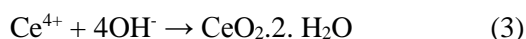
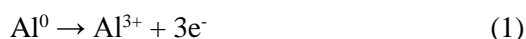
The present research work is investigation on the probabilities for application of a new cerium compound, for cathodic electrodeposition of Cerium based conversion coatings (CeCC) for protection of D16 AM alloy against corrosion. For the purpose of the present study, diammonium pentanitrocerate ((NH<sub>4</sub>)<sub>2</sub>Ce(NO<sub>3</sub>)<sub>5</sub>) was used, where the cerium is represented in the anionic moiety, instead of the electrolytes used up to nowadays. The barrier abilities against corrosion of all coatings were evaluated by two electrochemical methods – Linear Sweep Voltammetry (LSV), and Electrochemical Impedance Spectroscopy (EIS). Additionally, selected specimens underwent morphological characterization by Scanning Electron Microscopy (SEM) combined with Energy Dispersive X-ray spectroscopy (EDX). As a result, the influences of the concentrations of the basic substance and the deposition activator, as well as the density of the applied electric current were elucidated.

**Key words:** corrosion protection, Cerium Conversion Coatings, LSV, EIS, SEM, AFM

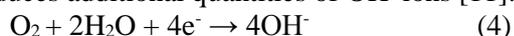
### INTRODUCTION

The aluminium alloys, especially, AA2024 and AA7075 are objects of special attention, due to their remarkable mechanical strength [1], predetermining their tremendous importance so for the commercial [2], so for military [3 - 6] aircraft, and recently, for the automotive [7, 8] industries. For industrial applications, the alloys are usually coated prior to their use as components for various transport vehicles and equipment. In the aircraft industry, it is commonly accepted to apply multilayered, multifunctional coatings [9].

The Cerium Conversion Coatings (CeCC) are generally composed by cerium oxides and hydroxides, originated from the conversion of the respective water-soluble cerium salts, according to the following reactions [10]:



The dissolved oxygen in the solution also could participate in reactions, and being reduced, it produces additional quantities of OH<sup>-</sup> ions [11]:



All these reactions lead to formation of insoluble

products of Cerium oxides or/and hydroxides. Here should be mentioned that according to the conditions, these products could form either precipitates (undesirable product), or layer deposition (the aimed product).

The aim of the present research work is to elucidate the influence of the addition of H<sub>2</sub>O<sub>2</sub> and the current applied as enhancers of the deposition process, by evaluation of the features and performance of the respective CeCC in 3.5% NaCl model corrosive medium.

### EXPERIMENTAL

The basic material was D16 AM clad alloy, with analogical composition to AA2024. For confirmation of its content, Inductively Coupled Plasma Optical Emission Spectroscopy (ICP-OES) was performed in the Central Laboratory of Scientific Research “Geohimia”, to “Ivan Rilsky” University of Mining and Geology. The composition determined is represented in Table 1.

Prior to CeCC deposition, the D16 AM substrates with 60x60x4 mm of size dimensions were submitted to: mechanical grinding with emery papers, up to 1200 grit, cleaning in acetone for 10 min at room temperature, and at last, alkaline etching in NaOH solution (50 g/l) at 55 °C for 5 minutes. Finally, the specimens underwent activation in diluted HNO<sub>3</sub> (1:1) for 5 minutes, at ambient temperature.

\* To whom all correspondence should be sent:  
E-mail: stephko1980@abv.bg

**Table 1.** Composition of the investigated alloy according to ICP – OES analysis

Element	Al	Cu	Fe	Mg	Mn	Ni	Si
Concentration (wt.%)	Residual	3.716	0.404	1.259	0.537	0.055	< 0.01

The basic substance was 0.05M  $(\text{NH}_4)_2\text{Ce}(\text{NO}_3)_5$  in the conversion bath solution, and presence of 10, 25, 50 or 100ml/l. of 30%  $\text{H}_2\text{O}_2$ . The depositions were performed at Galvani-static regime for 5 minutes either at -2 or at -5 mA/cm<sup>2</sup>. In order to compare the barrier abilities of the coatings, obtained after different additions of  $\text{H}_2\text{O}_2$ , electrochemical measurements were performed after 24 hours of exposition to 3.5% NaCl model corrosive medium.

The electrochemical procedures were performed by PG-stat, “Autolab”- 30, coupled by Frequency Response Analyzer FRA – 2.

The depositions and electrochemical characterizations were performed in flat cells with Ag/AgCl electrode and a platinum net as a counter electrode, and 100 ml of volume. In order to avoid the influence of the edge-effects on the measurements, the areas for deposition were larger than these for testing. Thus, the depositions were performed on circuit areas with diameter equal to 39 mm, whereas the tests were executed on areas with 15 mm. of diameter. The depositions and the tests were performed in the cells shown in Figure 1.

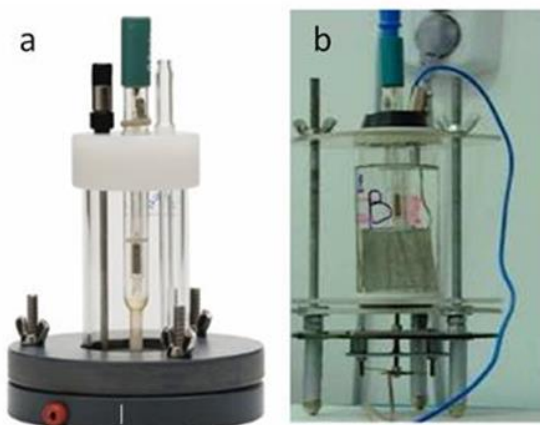


**Fig. 1.** Photographs of deposition (a), and test (b) cells

After 24 hours of exposition to 3.5% w/w. NaCl solutions, the respective impedance spectra were acquired at frequency range from  $10^4$  to  $10^{-2}$  Hz, distributed in 7 frequencies per decade, with signal amplitude of 10 mV vs. OCP. At last, individual cathodic and anodic polarization curves were recorded in a larger potential interval (OCP  $\pm$  500 mV), at 1 mV/s potential sweep range. The anodic curves were recorded after restoration of the OCP, deviated by the respective cathodic ones. By maintenance of this sequence, no disgrace of the

experimental data as a consequence of any electrode polarization could be admitted.

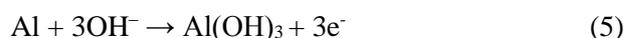
## RESULTS AND DISCUSSION

### *Chrono-potentiometric curves*

During the deposition, the equipment was continuously measuring the potentials versus the Ag/AgCl reference electrode and their evolutions within the deposition process. The obtained potential/time diagrams are shown in Fig. 2.

There, after the initial immediate fall of the potential down to almost -1.65 V, the potential reverses its values reaching about -1.30 to -1.32 V. The initial potential drop is related to the current spent for hydrogen evolution on the metallic surface. This process appears due to both of the reducing role of the cathodic current, and the generally acidic character of the deposition solution.

The subsequent reversion of the potential is probably related to removal of the  $\text{H}_2$  – gaseous bubbles from the metallic surface. Probably the reason for this removal and the reversion of the potential is the so called “cathodic dissolution of the aluminium” [12-15]. The peculiarities of the corrosion damage to cathodically polarized aluminum in aqueous solutions of different composition cannot be explained by the electrochemical process in which only the anodes should be dissolved [12, 13]. The most probable reaction is a chemical attack by hydroxyl ions (product of reactions (2) and (4)) on the aluminium cathode [13]. This process proceeds according to the following reactions [14, 15]:



The most extended continuation of the potential reversing is observable for the samples prepared with 100 and 50 ml/l  $\text{H}_2\text{O}_2$  (175 seconds for curve 1, and 125 seconds for curve 2). The curves 3 and 4 of the samples with more uniform, dense and homogeneous Ce-coatings achieve a minimum after 10 - 15 seconds.

After reaching maxima the potentials start to reverse gradually again for all curves. This phenomenon is related either to gradual growth of uniform coatings (curves 3 and 4), or to occupation of the metallic surface by cerium containing agglomerates.

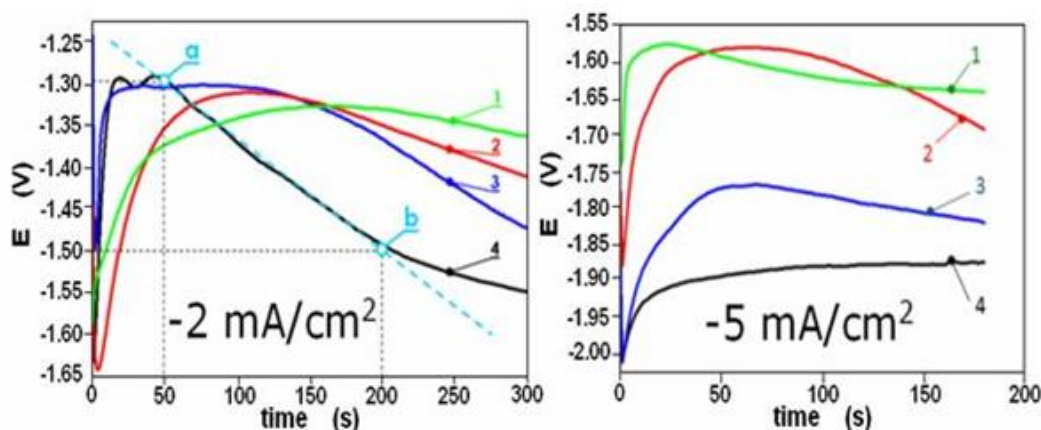


**Fig. 2.** Chronopotentiometric curves obtained during the Galvani-static depositions of CeCC coatings after different additions of H<sub>2</sub>O<sub>2</sub> to the coating solutions: 1 – 100ml/l H<sub>2</sub>O<sub>2</sub>; 2 - 50 – 10ml/l H<sub>2</sub>O<sub>2</sub>; 3 – 25ml/l H<sub>2</sub>O<sub>2</sub>; 4 - 10ml/l H<sub>2</sub>O<sub>2</sub>.

For the best coating, obtained by addition of only 10 ml/l. H<sub>2</sub>O<sub>2</sub>, this gradual drop of potential continued from the 50<sup>th</sup> (point (a)) to 200<sup>th</sup> (point (b)) second after the beginning of the deposition. During this time, the potential drops with 200 mV. Taking into account that the deposition is performed in Galvani-static regime (i.e: -2 mA/cm<sup>2</sup>) and, applying the law of Ohm, it could be calculated that the resistance of the deposited film increases with 100 Ω.cm<sup>2</sup>/s. In other words, for the entire period of film growth (between points (a) and (b)) the total resistance of the best film (curve 1) raises up to 15 k Ω.cm<sup>2</sup>). As a general conclusion, it looks that the increase of the H<sub>2</sub>O<sub>2</sub> content in the deposition solutions probably favors the cathodic dissolution of the underlying aluminum, hindering the formation of uniform and homogeneous CeCC coatings.

The curves, obtained during the electrodeposition at -5 mA/cm<sup>2</sup> do not possess the slope related to film growth. Consequently, at this current density, any uniform and homogeneous coating layer does not form (Fig. 2). It either favors the hydrogen evolution process, or promotes the mentioned above cathodic Al-dissolution. In both cases, the acquired coatings possess elevated porosity, or lower homogeneity.

#### EIS – examination

After the depositions, the obtained samples were exposed to 3.5 %NaCl model corrosive media. Their barrier abilities were examined by means of electrochemical measurements (EIS, and LSV). Unexpectedly, the addition of oxidant has not presented its contribution in the impedance spectra. In Fig. 3 (a, b), all of the spectra of the coatings obtained at -2mA/cm<sup>2</sup> possess almost the same shapes, regardless the significant difference of the

H<sub>2</sub>O<sub>2</sub> additions to the solution of the conversion bath.

For the EIS – spectra of the samples with films deposited at -5 mA/cm<sup>2</sup>, also cannot be seen any significant difference among the shapes in Bode plots. However, when the Nyquist plots of Fig. 3 (b, d) are compared, clear Warburg diffusion elements are observable in the latter position (e. g: at -5 mA/cm<sup>2</sup>). This fact evinces that the higher deposition currents applied result in formation of rather less uniform deposits. Indeed, the visual inspections of the samples revealed rough and grain-formed (agglomerated) precipitates, when the higher current was applied. The unsatisfying homogeneity of the coatings favors the access of corrosive species to the metallic surface, resulting in appearance of the Warburg diffusion impedance.

#### LSV – measurements

The linear voltammograms reveal more distinguishable features of the respective specimens, than the EIS spectra. Fig. 4 represents cathodic (a, c) and anodic (b, d) polarization curves of specimens coated after different H<sub>2</sub>O<sub>2</sub> additions, and current densities, recorded after 24 hours of exposition to the model corrosive medium. Fig. 4, (a, b) reveals that for the coatings deposited at -2 mA/cm<sup>2</sup>, the increase of the H<sub>2</sub>O<sub>2</sub> content deteriorates the barrier ability of the resulting coatings. Thus, the coatings prepared at lower content of the oxidant (10 and 25 ml. 30% H<sub>2</sub>O<sub>2</sub> per liter of coating solution), resemble lower current densities, compared to the other two (50 and 100 ml. 30% H<sub>2</sub>O<sub>2</sub> per liter of coating solution). The anodic curve of the sample, prepared at 50 ml./l. H<sub>2</sub>O<sub>2</sub>, does not possess any passivity region. Both curves of the sample with 100 ml. H<sub>2</sub>O<sub>2</sub> addition stay at lower current

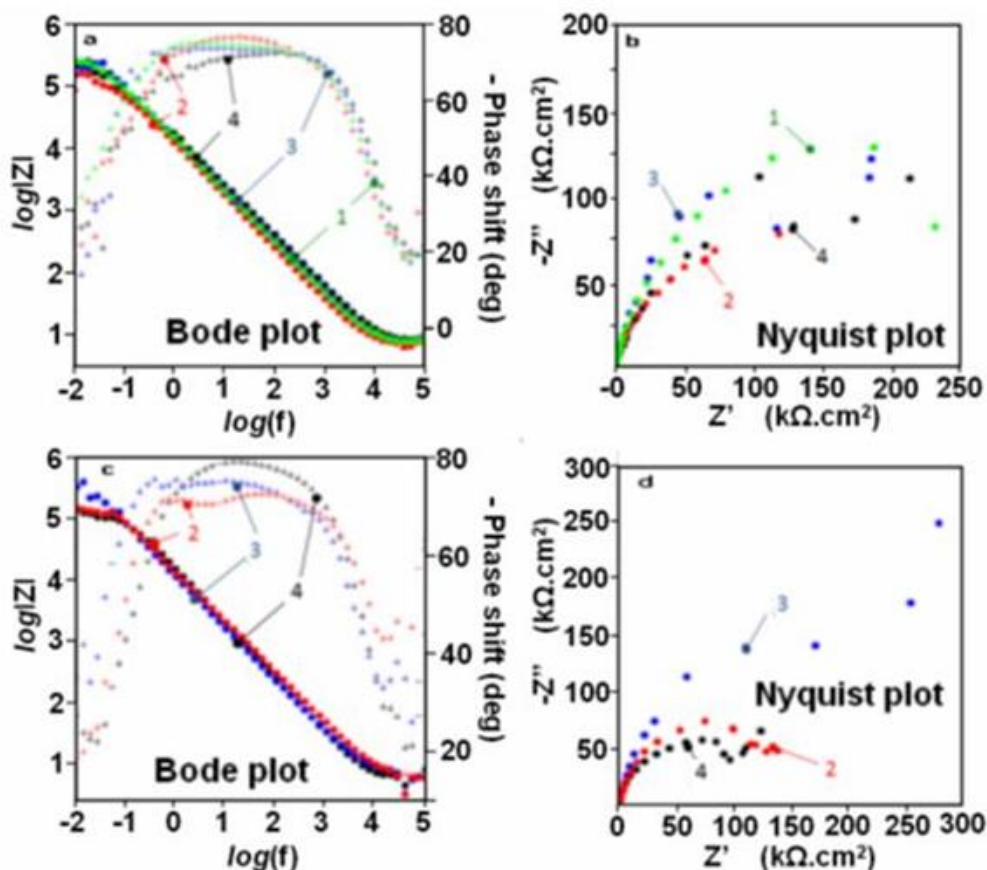


**Fig. 3.** Electrochemical impedance spectra, acquired after 24 hours of exposition to the model corrosive medium of four specimens coated after different  $\text{H}_2\text{O}_2$  additions. a, c – Bode plots; b, d – Nyquist plots: 1 – 100ml/l addition of  $\text{H}_2\text{O}_2$ ; 2 – 50 – 10ml/l addition of  $\text{H}_2\text{O}_2$ ; 3 – 25ml/l addition of  $\text{H}_2\text{O}_2$ ; 4 – 10ml/l addition of  $\text{H}_2\text{O}_2$

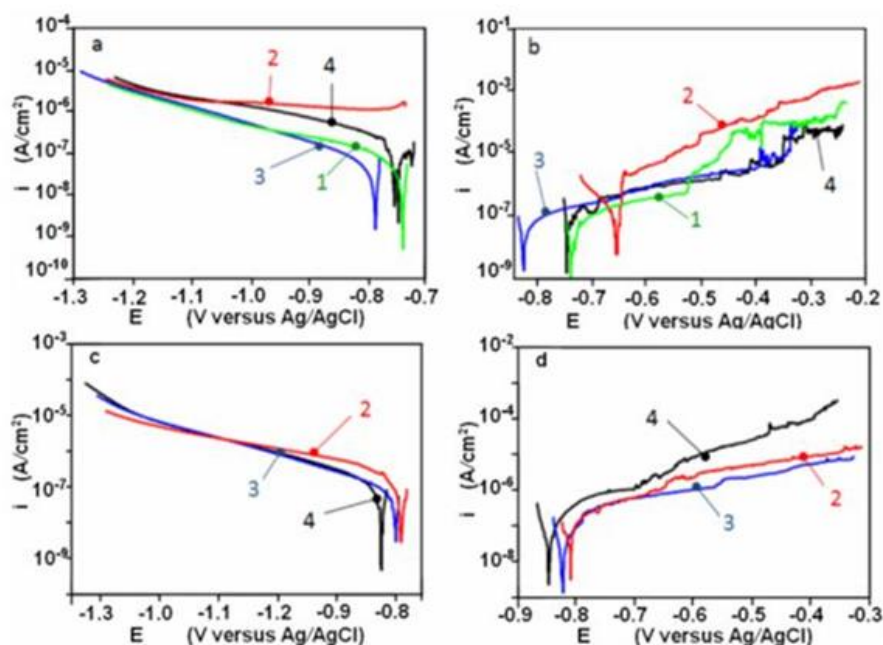


**Fig. 4.** Cathodic (a, c) and anodic (b, d) polarization curves recorded after 24 hours of exposition to the model corrosive medium of specimens coated at  $-2\text{mA}/\text{cm}^2$  (a,b) and  $-5\text{mA}/\text{cm}^2$  (c, d) after different  $\text{H}_2\text{O}_2$  additions. 1 – 100ml/l addition of  $\text{H}_2\text{O}_2$ ; 2 – 50ml/l addition of  $\text{H}_2\text{O}_2$ ; 3 – 25ml/l addition of  $\text{H}_2\text{O}_2$ ; 4 – 10ml/l addition of  $\text{H}_2\text{O}_2$

densities, than these of the sample coated after 50 ml.  $H_2O_2$  addition. Nevertheless, the respective anodic curve (of the sample with 100 ml.  $H_2O_2$ ) has shorter region of passivity (from -750 to -550 mV) than the curves of the samples with lower  $H_2O_2$  additions. According Bethencourt and co. [16], the shorter passivity regions indicate lower strength against pitting nucleation.

Between the samples, prepared at lower  $H_2O_2$  content, the cathodic curve of the sample prepared after 25 ml / l.  $H_2O_2$  addition, stays at lower current densities, than this of the sample with 10 ml. However, the respective anodic curves stay at the same current densities, revealing very similar barrier ability. Furthermore, the curve of the sample with 10 ml. oxidant addition have relatively larger passivity region. From these relatively equivocal features of the polarization curves, could be concluded that the optimal addition of peroxide should be in the range of 10 and 25 ml. 30%  $H_2O_2$  for liter of conversion bath.

Fig. 4 (c, d) reveals that at  $-5mA/cm^2$ , the voltammograms of the samples with different  $H_2O_2$  additions are less distinguishable, compared to those, deposited at lower current densities. This phenomenon could be explained, having in mind that the deposition current plays a role of reducer. As a result, at higher current densities ( $-5mA/cm^2$ ), the influence of the  $H_2O_2$  as oxidant is less notable.

The supply of charged particles towards the specimen (by the electric current) leads to deactivation of the peroxide by obtaining of  $OH^-$  ions (equation 2) and acceleration of oxygen reduction (equation 4). Both these processes result in alkalisation of the medium near the substrate surface and acceleration of Ce-precipitation (equation 3).

However, the obtained  $Ce(OH)_3/Ce(OH)_4$  precipitates do not form a coating layer, but rather conjunction of clusters.

#### *Superficial morphological observations*

Following the literature [10], the increase of the oxidant content should accelerate the coating deposition. Consequently, it is expectable to improve the density and barrier ability of the coating after increase of  $H_2O_2$  addition. Nevertheless, it was observed that the elevated content of peroxide has detrimental effect on the homogeneity and uniformity of the obtained coatings. As could be seen in Fig. 5, all the samples prepared with elevated additions of  $H_2O_2$  have not uniform coatings, but rather they are covered by rough aggregates. Furthermore, these aggregates did not possess almost any adherence to the metallic substrates, so that metallic shining under the Ce-deposits was clearly observable, as a result of partial removal of the Ce-containing aggregates.

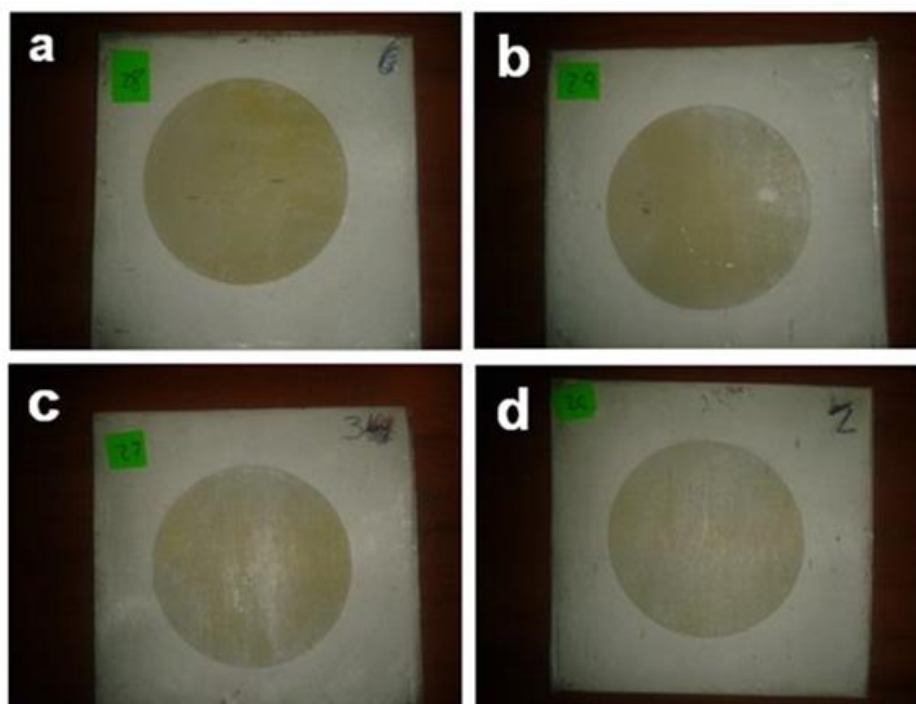


**Fig. 5.** Photographs of four samples with coatings, deposited after different additions of oxidant: a – 10ml/l addition of  $H_2O_2$ ; b - 25ml/l addition of  $H_2O_2$ ; b - 50ml/l addition of  $H_2O_2$ ; d - 100ml/l addition of  $H_2O_2$ ;

The CeCCs, deposited at  $-5\text{mA}/\text{cm}^2$  generally reveal inferior features than those with CeCC electrodeposited at  $-2\text{mA}/\text{cm}^2$ .

In order to observe the morphology of the coating, Scanning Electronic Microscopy (SEM), combined by energy dispersion X-ray analysis were applied on the best samples before and after 168 hours of exposition to naturally aerated 3.5% NaCl model corrosive medium. These coatings possess peculiar features. Larger oval hills are clearly distinguishable on the surfaces. Probably these sides are locations of preferential deposition of the layer, as was observed in previous works [17-21]. Consequently, these oval hills are formed as consequence of preferential deposition on intermetallics.

- *EDX analysis* – In order to clarify the real composition of the samples, and the distribution of the elements on their surfaces, EDX – map analyses were executed during the SEM observations. The next figure represents the elemental distributions of the most important chemical elements: Al, Ce, Cu, and oxygen. These elements were selected because the aluminium could be presented not only from the metallic substrate, but also to compose corrosion

products, in form of  $\text{Al}(\text{OH})_3$ , etc. The cerium was selected because this element together with the oxygen is the basic components of the coating. The copper was also selected to be monitored, because it should reveal whether the S-phases are preferable locations of deposition, and is there a copper re-deposition as evidence of corrosion during the deposition. Fig. 6 shows EDX –map data and SEM image of CeCC, obtained by deposition for 5 min. from 0.05 M  $(\text{NH}_4)_2\text{Ce}(\text{NO}_3)_5$  with 10ml/l addition of 30%  $\text{H}_2\text{O}_2$ .

The Al-distribution map in Fig. 6 reveals that there is aluminum deposited on the coating. It is undoubtedly originated from corrosion products formed during the deposition. The EDX-map of cerium shows that the sides of preferable deposits coincide with the highest abundance of cerium. Nevertheless, there is uniform distribution of this element on the rest part of the coated surface. The copper is also equally distributed on the metallic surface. This fact is consequence and indication of copper re-distribution. This process passes because of the cathodic Al-dissolution of the metallic matrix.

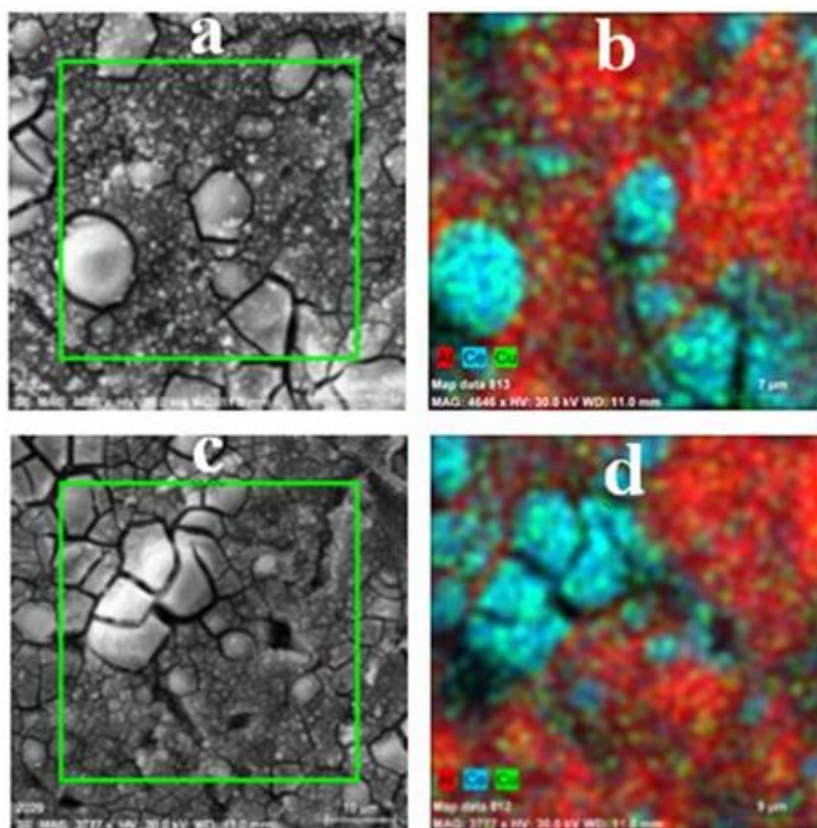


**Fig. 6.** SEM images (a, c), and EDX map data (b, d) of sample after prepared by deposition for 5 min. from 0.05 M  $(\text{NH}_4)_2\text{Ce}(\text{NO}_3)_5$  with 10ml/l addition of  $\text{H}_2\text{O}_2$

## CONCLUSION

As a result of the investigations performed, the following conclusions are done:

Diammonium pentanitrocerate was used as provider of Ce-ions during the coating deposition. In this substance, the Ce is presented in the anionic compositional part in difference of the widely used  $\text{CeCl}_3$ , or  $\text{Ce}(\text{NO}_3)_3$ .

It is found that at different concentrations of  $(\text{NH}_4)_2\text{Ce}(\text{NO}_3)_5$  in range 0.01 to 0.1 moles per liter, the optimal concentration is about 0.05 M  $(\text{NH}_4)_2\text{Ce}(\text{NO}_3)_5$ .

It is determined that the optimal content of peroxide is in the range of 10 and 25 ml/l. of 30%  $\text{H}_2\text{O}_2$  for the investigated system.

It is established that the best CeCC were electrodeposited at  $i = -2\text{mA}/\text{cm}^2$  current density and 5 minutes.

It was determined by SEM observations that the morphology of the coating does not repeat those of the metallic substrate, showing complete coverage by the coating.

The Cerium conversion coatings elaborated in the present research work could serve as a basis for future coating systems.

**Acknowledgements:** The authors gratefully acknowledge the financial support of project BG 051PO001-3.3.06-0038. Dr. Gustavo Pelaez is acknowledged for the opportunity for the international collaboration activities.

## REFERENCES

1. E.A. Starke and J. T. Staley, *Prog. Aerospace Sci.* **32**, 131 (1996).
2. AIRBUS A380, *Airplane characteristics*, Issue 30.03.05 (2005), [www.content.airbusworld.com/SITES/Technical.../A\\_C\\_A380.pdf](http://www.content.airbusworld.com/SITES/Technical.../A_C_A380.pdf)
3. M. J. O'Keefe, S. Geng, S. Joshi, *Metalfinishing* (2007) 25 – 28
4. S. Geng, S. Joshi, W. Pinc, W.G. Fahrenholtz, (1)M.J. O'Keefe, T.J. O'Keefe, and P. Yu "Influence of processing parameters on cerium based conversion coatings" Proceed "TRI – Service – 2007" - corrosion conference: Accessible via: <https://www.corrdefense.org/Technical%20Papers/Influence%20of%20Processing%20Parameters%20on%20Cerium%20Based%20Conversion%20Coatings.pdf>
5. B. Hindin "Corrosion protection of aluminium alloys by corrosion prevention compounds as measured by electrochemical techniques" accessible via: <https://www.corrdefense.org/Academia%20Government%20and%20Industry/XVIII%20-%20HINDIN%20-%20Corrosion%20Protection%20of%20Aluminum%20Alloys%20by.pdf>
6. P. Ostash, I. M. Andreiko, Yu. V. Holovatyuk, O. I. Semenets, *Mater. Sci.* **44**, 672 (2008).
7. J.A. Rodríguez-Martínez, A. Rusinek, A. Arias, Thermo-Viscoplastic behaviour of AA2024 aluminium sheets subjected to low velocity perforation at different temperatures, accessible via: [http://e-archivo.uc3m.es/bitstream/10016/11941/1/rodriguez\\_thermo\\_TWS\\_2011\\_ps.pdf](http://e-archivo.uc3m.es/bitstream/10016/11941/1/rodriguez_thermo_TWS_2011_ps.pdf)
8. Y. Komatsu, New Pretreatment and Painting Technology for All Aluminum Automotive Body, paper no. 910787, SAE Technical Paper Series-International Congress/AIRP Meeting (Warrendale, PA: SAE International, 1991).
9. G. Tsaneva, V. Kozhukharov, S. Kozhukharova, M. Ivanova, J. Gerwann, M. Schem, T. Schmidt, *J. Univ. Chem. Technol. Met.*, **43**, 231 (2008).
10. M. J. O'Keefe, S. Geng, S. Joshi, *Metalfinishing*, 25 (2007).
11. K. A. Yasakau, M. L. Zheludkevich, S. V. Lamaka, M. G. S. Ferreira, *J. Phys. Chem.*, **B- 110**, 5515 (2006).
12. M. D. Tkalenko, *Protection of Metals*, **37(4)**, 301, (2001).
13. T. Picard, G. Cathalifaud-Feuillade, M. Mazet, C. Vandesteendam, *J. Environ. Monit.* **2(1)**, 77 (2000).
14. M. Mokaddem, P. Volovitch, F. Rechou, R. Oltra, K. Ogle, *Electrochim. Acta*, **55**, 3779 (2010).
15. S. K. Ogle, M. Serdechnova, M. Mokaddem, P. Volovitch, *Electrochim. Acta*, **56**, 1711 (2011).
16. M. Bethencourt, F.J. Botana, M.J. Cano, M. Marcos, J.M. Sánchez-Amaya, L. González-Rovira, *Corros. Sci.* **51**, 518 (2009).
17. J. E. Pernas, S. Kozhukharov, A. A. Salve, E. A. Matter, M. Machkova, *J. Univ. Chem. Technol. Met.*, **47**, 311 (2012).
18. E. A. Matter, S. Kozhukharov, M. Machkova, V. Kozhukharov, *Mater. Corros.*, DOI: 10.1002/maco.201106349
19. E. A. Matter, S. Kozhukharov, M. Machkova, V. Kozhukharov, *Corros. Sci.* **62**, 22 (2012).
20. E. Matter, S. Kozhukharov, M. Machkova, SEM and EDS determination of the impact of inhibitor containing corrosive media over the AA2024 superficial morphology, Ann. Proc. of "Angel Kanchev" – University of Rousse (Bulgaria), **50**, 60, (2011). Accessible via: <http://conf.uni-rouse.bg/bg/docs/cp11/9.1/9.1-10.pdf>
21. M. Machkova, E.A. Matter, S. Kozhukharov, V. Kozhukharov, *Corros. Sci.*, **69**, 396 (2013).

## ЕЛЕКТРОХИМИЧНО ОТЛАГАНЕ НА ЦЕРИЕВИ КОНВЕРСИОННИ ПОКРИТИЯ ЗА КОРОЗИОННА ЗАЩИТА НА ПЛАКИРАНА СПЛАВ Д16 АМ

Х. А. П. Айюсо<sup>1</sup>, С. Кожухаров<sup>2\*</sup>, М. Мачкова<sup>2</sup>, В. Кожухаров<sup>2</sup>

<sup>1</sup>Университет Виго, Лагоас Марконсенде 36310 (Испания)

<sup>2</sup>Химикотехнологичен и Металургичен Университет, бул. "Климент Охридски" № 8 София 1756 (Б)

Постъпила на 31 януари, 2013 г.; Коригирана на 21 май, 2013 г.

(Резюме)

Настоящата работа представя изследване върху възможностите за използване на ново цериево съединение за катодно електрохимично отлагане на цериево-основани конверсионни покрития (ЦКП) за защита на плакирана сплав Д16 АМ против корозия. За целите на настоящето изследване беше използван диамониев пентанитроцерат  $((\text{NH}_4)_2\text{Ce}(\text{NO}_3)_5$ , при който церият е представен в анионната съставна част на съединението, за разлика от електролитите, използвани до сега. Бариерната способност против корозионна атака на всички изследвани образци в настоящата работа беше оценена по два различни електрохимични метода: Волтаперометрия с Литнейна Разгъвка на Потенциала (ВЛРП) и Електрохимична Импедансна Спектроскопия (СЕМ). В допълнение, избрани образци преминаха морфологично описание чрез Сканираща Електронна Микроскопия (СЕМ), съчетана с Енергийно Разпределителна Рентгенова Спектроскопия (ЕРРС). Като резултат, беше оценено въздействието на концентрациите на основното вещество и активатора за отлагане, както и плътността на приложения ток.